MODELING AND SIMULATION OF POWER HACKSAW MACHINE USING BOND GRAPH

Anand Vaz[(a)], Aman Maini[(b)]

[(a)] Department of Mechanical Engineering, Dr. B.R. Ambedkar National Institute of Technology, Jalandhar
[(b)] Department of Mechanical Engineering, DAV Institute of Engineering & Technology, Jalandhar

[(a)]anandvaz@ieee.org, [(b)]er_maini@yahoo.co.in

ABSTRACT
The mechanism of a machine involves a number of interconnected rigid bodies which interact with each other dynamically. Formulations of dynamics for such mechanisms available in literature, usually either do not reveal the physical aspects involved, or tend to be too mathematically inclined. Aspects of cause and effect are also obscured. In this paper, the multibond graph approach is used as an alternative but powerful method, for modeling the dynamics of mechanisms taking the specific example of a power hacksaw machine, which is quite common in industry. The mechanism is modeled as a combination of rigid links suitably constrained at joints. Bond graph offers the capability for pictorial representation of the dynamics of mechanisms, based on interaction of power between elements, and also depicts the cause and effect relationships. Coding for simulation can be done directly from the multibond graph without deriving system equations. In this work, the program coding is implemented in MATLAB. The simulation results are analyzed, plotted and discussed.

Keywords: Modeling, simulation, power hacksaw mechanism and Bond Graph.

1. INTRODUCTION

The mechanism of a machine involves a number of interconnected rigid bodies which interact with each other dynamically. Kinematics of such mechanisms is presented in most books on machines and mechanisms but the dynamics is rarely available. Modeling the dynamics of mechanisms is also necessary from the point of view of design, analysis and control. The dynamics of such mechanisms can be described using a number of formalized procedures like the Newton-Euler, Lagrange-Euler, Kane's dynamics etc (Fu, Gonzalez and Lee 1986; Murray, Li, and Sastry 1993). These formulations usually either do not reveal the physical aspects involved, or tend to be too mathematically inclined. Aspects of cause and effect are also obscured. The technique of Bond graph modeling successfully overcomes the difficulties encountered, and also provides several significant advantages not provided by the conventional formulation techniques (Karnopp, Margolis, and Rosenberg 2000). The Bond Graph technique has become widely accepted and several software tools are now commercially available for Bond graph modeling and simulation.

The Bond graph technique is especially convenient and computationally advantageous for dynamic analysis of mechanisms. Bond graph is the pictorial representation of the dynamics of the system and is convenient for modeling of physical system dynamics in multiple energy domains. It offers a unified framework for modeling the mechanism, and, the actuation and control systems due to its capability of handling multi-energy domains. The application of this technique results in a number of advantages. In addition, depiction of causality in Bond graph shows the *cause* and *effect* relationship between the *flow* and *effort* elements of the bond. The notion of causality, apart from aiding with the formulation of system equations which govern the behavior of the system, help in pointing out any physical impossibility or system property that may have failed to be taken into account at the modeling stage. Software are commercially available for multibody dynamics simulation. However, these do not offer sufficient freedom to the user to incorporate modeling of additional physical phenomena, actuator dynamics, fault diagnostics, or scope for study of *cause* and *effect*.

Multibond graph modeling of rigid body based mechanisms have been discussed in (Bos and Tiernego 1985; Tiernego and Bos 1985). Formulation of rotational dynamics in the inertial frame using multibond graphs has been presented in (Vaz and Hirai 2004; Vaz and Thommen 2010), and the computational advantages elaborated in (Vaz 2008). Ersal et al. (2004) have discussed multibond graph based formulations as applied to machine tool mechanisms.

In this paper, the multibond graph approach is used as an alternative but powerful method, for modeling the dynamics of mechanisms taking the specific example of a power hacksaw machine, which is quite common in industry (Norton 1996). The mechanism of power hacksaw machine offers an opportunity to demonstrate modeling of revolute as well as prismatic joints, and also the interface of the machine with work piece during the cutting operation. The power hacksaw mechanism is modeled as a combination of five rigid links suitably constrained at joints, having relative movement with each other.

Reference frames are fixed on each link using the Denavit-Hartenberg convention (Craig 2005). Usually, the translational dynamics of a link is considered in the inertial frame and rotational dynamics is expressed in the moving frame fixed on the moving link. In this paper, both the translational and rotational dynamics are expressed in the inertial frame, as discussed in (Vaz and Hirai 2004, Vaz 2008). The computational advantages due to this formulation, therefore, have not been discussed again in this paper.

The problem of differential causality arises due to constraints imposed at joints; suitable stiffness and damping elements are added for rectifying this problem and converting the model into one with complete integral causality. These elements make the model more realistic by bringing in the effects of compliance and dissipation at the joints, within definable tolerance limits. At the interface between the cutting blade and work-piece, the resistive forces are different during forward stroke and cutting stroke which is in the backward direction.

Coding for simulation is done directly from the multibond graph without deriving system equations. In this work, the program coding is implemented using MATLAB (2010). Important dynamic quantities like reaction forces and torques at various joints on the system can be determined, plotted and analyzed. The simulation results are analysed, plotted and discussed.

2. MODELING

In this work, a multibond graph model of power hacksaw machine is developed. The mechanism is considered as a combination of five rigid links connected at joints. There is relative movement of links with each other and also with inertial frame. Frame *1* which is a fixed frame, is taken as inertial frame. The *0* frame and *1* frame coincide with each other. This inertial frame does not possess any translational or rotational motion. The power hacksaw machine is used for metal cutting in industries. The mechanism involves five rigid links; link *1* is taken as the fixed frame, link *2* is the crank which is connected to connecting rod (link *3*). The connecting rod is connected to the frame (link *4*), in which the cutting blade is adjusted. The link *4* has sliding motion in guide link *5*. The link *5* has revolute movement about origin O_5. The origin is assigned as O_1, O_2 and O_5 to link *1*, link *2* and link *5*. The mass of the link *5* is more than link *4*. The link *5* applies force due to gravity on link *4* resulting in downward movement of link *4*, so that during cutting operation the cut may proceed in the downward direction. C_1, C_2, C_3, C_4 and C_5 are center of masses of respective links.

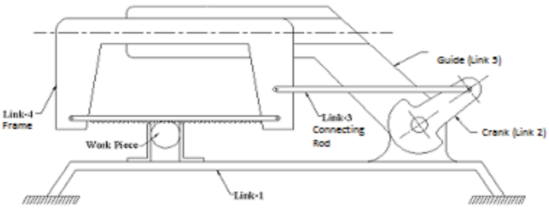

Fig. 1: The power Hacksaw machine

The dynamics of the system is modeled using multibond graph. The bond graph of the system is shown in Fig. 3. The thick lines in bond graph represent the multibonds while the thin lines show scalar bonds. The left side of the bond graph is associated with the rotational dynamics of the model while the right side shows the translational dynamics. The translational motion of the crank is restricted by applying S_f equal to zero between O_1 and O_2 ; the origin of fixed frame and that of frame *2* respectively. The relative movement between links at each origin is distinguished such as the point A_2 on link *2* and point A_3 on link *3*. Point B_3 on link *3* and B_4 on link *4*.

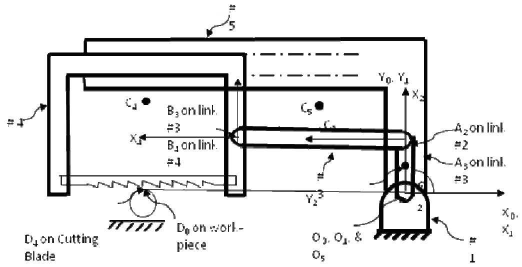

Fig. 2: The Power Hacksaw Machine (link diagram)

To eliminate the differential causality, viscoelastic elements introducing stiffness and damping are provided at revolute joints such as at the joint of frame and crank (link *1* and link *2*) stiffness *C:* k_{2r} and damping *R:* r_{2r} at the joint of crank and connecting rod the stiffness C: k_{23r} and damping *R:* r_{23r} and at the joint of connecting rod and frame *4* the stiffness *C:* k_{34r} and *R:* r_{34r} are applied.

For simulation, a torque of 10 *N·m* is applied at the crank. The crank is made to rotate about point O_1 (about *Z*-axis). The movement of the crank in other two directions (*X* and *Y* axis) is constrained by applying S_f equal to *0*. As the link *4* slides in the guide-way of link *5* so the relative angular movement between these two links is constrained equal to zero by equating S_f to *0*. At the interface of cutting blade and work-piece, point D_4 is taken at cutting blade (i.e. blade is fixed in frame *4*) while point D_0 is considered at work-piece. The distance of D_4 from O_1 remains fixed. Due to the reciprocating movement of frame *4*, the relative distance between center of mass (C_4) of link *4* and point D_4 changes during cutting operation. The blade slides in *X*-direction of frame *4* only, so the movement of blade in other two directions is constrained.

$$ {}^0_0\bar{r}_{D_0} = {}^0_{D_4}\bar{r}_{D_0} + {}^0_{C_4}\bar{r}_{D_4} + {}^0_0\bar{r}_{C_4} \quad (1) $$

Differentiating w.r.t. time *t*,

$$ {}^0_0\dot{\bar{r}}_{D_4} = {}^0_0\dot{\bar{r}}_{C_4} + \left[{}^0_0\bar{\omega}_4 \times \right] {}^0_{C_4}\bar{r}_{D_4} + {}^0_4R \, {}^4_{C_4}\dot{\bar{r}}_{D_4} \quad (2) $$

which can be written as,

$$ {}^0_0\dot{\bar{r}}_{D_4} = {}^0_0\dot{\bar{r}}_{C_4} - \left[{}^0_{C_4}\bar{r}_{D_4} \times \right] {}^0_0\bar{\omega}_4 + {}^0_4R \, {}^4_{C_4}\dot{\bar{r}}_{D_4} \quad (3) $$

${}^0_0\bar{r}_{D_0}$ is the position vector from Origin O_1 to point D_0 expressed in frame *0*. ${}^0_{D_4}\bar{r}_{D_0}$ is the position of the interface of cutting blade and work-piece from point C_4. ${}^0_{C_4}\bar{r}_{D_4}$ is the position vector from center of mass of link *4* and cutting point at blade. This distance changes during cutting operation. ${}^0_0\bar{r}_{C_4}$ is the distance of center of mass of link *4* from origin O_1. ${}^0_0\bar{\omega}_4$ is the angular velocity of blade frame *4*, w.r.t. frame *0* and is expressed in frame *0*. The Bond graph of Fig. 3 incorporates the kinematics of (3).

The translational effect is concentrated at the center of mass of each link, while the rotational effect is considered in the inertial frame itself by considering the inertia tensor for each link about its respective center of mass and expressed in the inertial frame. This implies that the inertia tensor changes continuously with orientation. However, this aspect has been taken into consideration, and requires lesser number of computations in terms of multiplications and additions (Vaz 2008).

3. SIMULATION RESULTS

The simulation has been performed in MATLAB. The parameters used are shown in Table 1. Table 2 represents the values of stiffness and damping at different couplings.

Table-1: Link properties used for simulation

Crank (Link *2*)			
	${}^2l_x = 0.075\ m$	${}^2l_y = 0.04\ m$	${}^2l_z = 0.02\ m$
Connecting Rod (Link 3)			
	${}^3l_x = 0.7\ m$	${}^3l_y = 0.04\ m$	${}^3l_y = 0.03\ m$
Frame (Link 4)			
	$a_{41} = 0.03\ m$	$b_{41} = 0.13\ m$	$c_{41} = 0.03\ m$
	$a_{42} = 0.03\ m$	$b_{42} = 0.13\ m$	$c_{42} = 0.03\ m$
	$a_{43} = 0.4\ m$	$b_{43} = 0.03\ m$	$c_{43} = 0.03\ m$
Guide (Link 5)			
	$a_{51} = 0.1\ m$	$b_{51} = 0.09\ m$	$c_{51} = 0.03\ m$
	$a_{52} = 0.09\ m$	$b_{52} = 0.7\ m$	$c_{52} = 0.03\ m$

Table- 2: Stiffness and damping of various couplings for simulation.

Location	Stiffness (K)	Damping (R)
Translational coupling between		
fixed frame and crank	$k_2 = 10^7$ *N/m*	$r_2 = 0.5$ *N-s/m*
crank and connecting rod	$k_{23} = 10^7$ *N/m*	$r_{23} = 10^2$ *N-s/m*
connecting rod and frame 4	$k_{34} = 10^8$ *N/m*	$r_{34} = 0.5$ *N-s/m*
fixed frame and guide 5	$k_{15} = 10^6$ *N/m*	$r_{15} = 10$ *N-s/m*
Rotational coupling between		
fixed frame and crank	$k_{2rx} = 10^3$ *N.m/rad* $k_{2ry} = 10^3$ *N.m/rad*	$r_{2rx} = 10^2$ *N.m.s/rad* $r_{2ry} = 10^2$ *N.m.s/rad*
crank and connecting rod	$k_{23rx} = 10^3$ *N.m/rad* $k_{23ry} = 10^3$ *N.m/rad*	$r_{23rx} = 10^2$ *N.m.s/rad* $r_{23ry} = 10^2$ *N.m.s/rad*
connecting rod and frame 4	$k_{34rx} = 10^3$ *N.m/rad* $k_{34ry} = 10^3$ *N.m/rad*	$r_{34rx} = 80$ *N.m.s/rad* $r_{34ry} = 80$ *N.m.s/rad*
frame 4 and Guide 5	$k_{45r} = 10^4$ *N.m/rad*	$r_{45r} = 100$ *N.m.s/rad*
Resistive Forces between cutting blade and work-piece.	$k_{Rfy} = 10^2$ *N/m* $k_{Rfz} = 10^2$ *N/m*	$r_{Rfx} = 10^2$ *N.m.s/rad* $r_{Rfy} = 10^2$ *N.m.s/rad* $r_{Rfz} = 10^2$ *N.m.s/rad*

3.1. Simulation graphs

The simulation plots for various links are shown in this section. The time span for simulation is taken as 5 seconds.

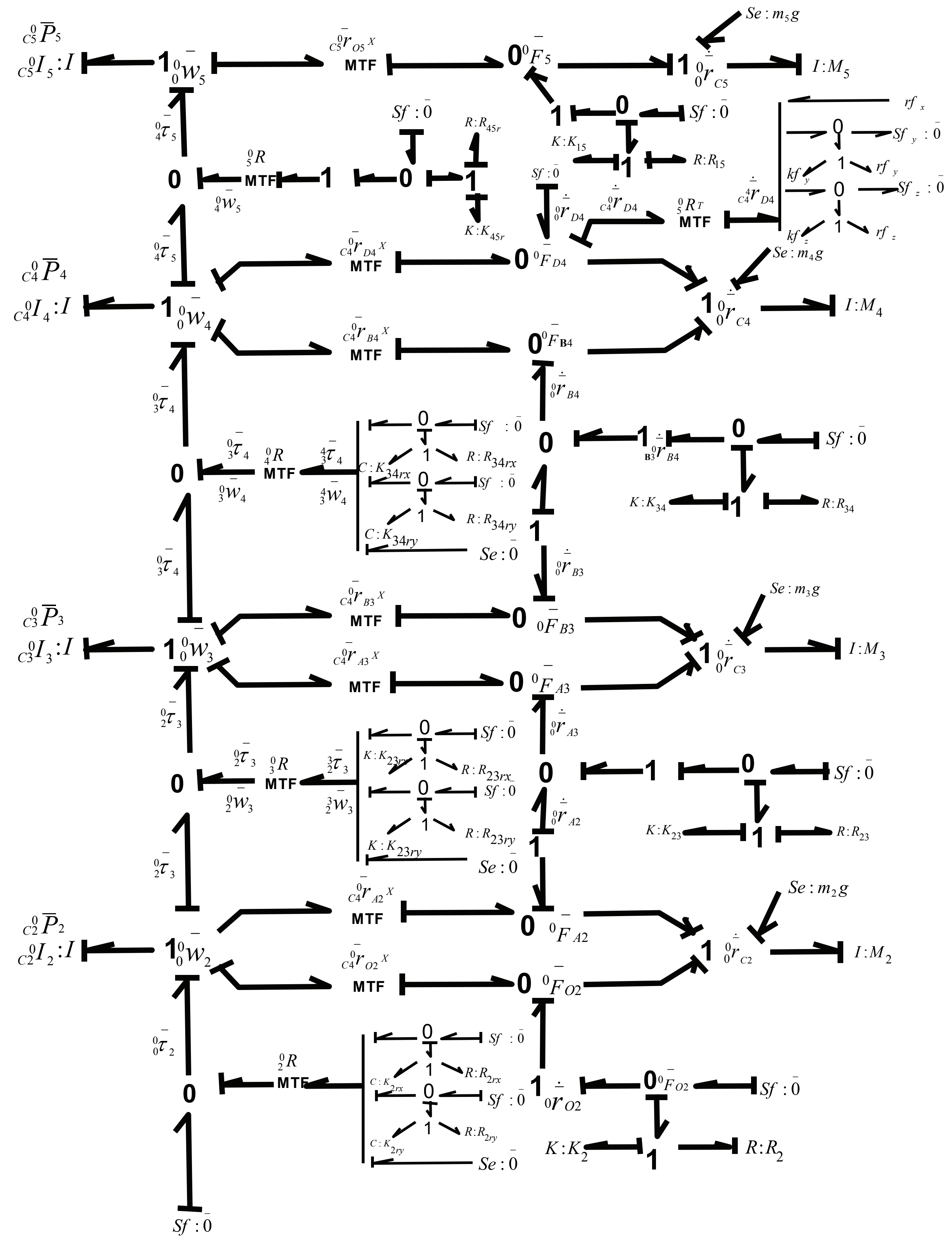

Fig.3: Bond Graph of Power Hacksaw Machine

3.1.1 Dynamics of the crank

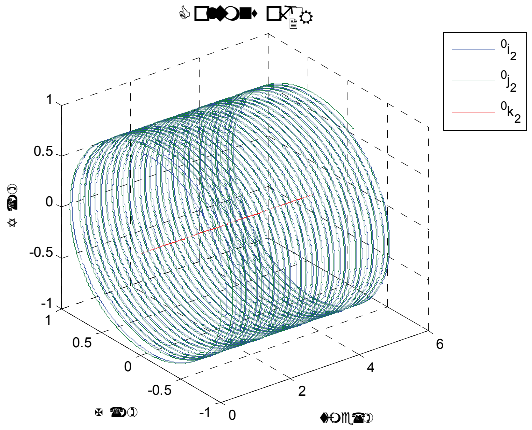

Fig. 4: Variation of orientation matrix of link *2* with time.

The link *2*, that is the crank, rotates about origin O_2. Hence in Fig. *4*, the unit vectors in *x* and *y* direction describe circular paths while that in the *z* direction is stationary.

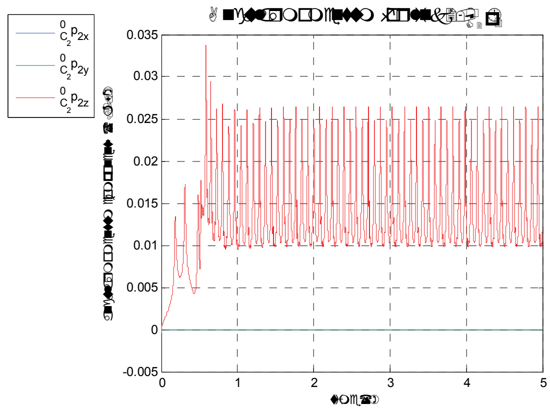

Fig. 5: Variation of angular momentum of link *2* with time.

In Fig. *5,* only the *Z* component of angular momentum varies. This is due to the constant torque applied at the crank.

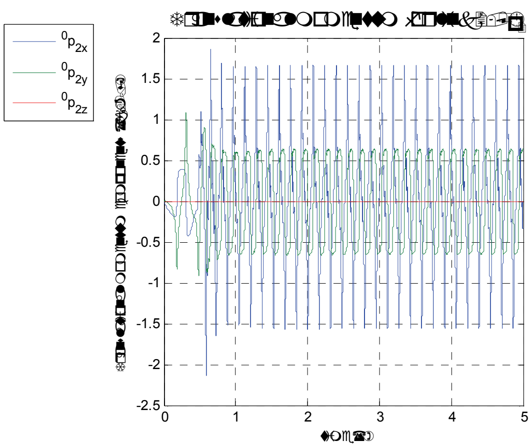

Fig. 6: Variation of Translational momentum of link *2* with time.

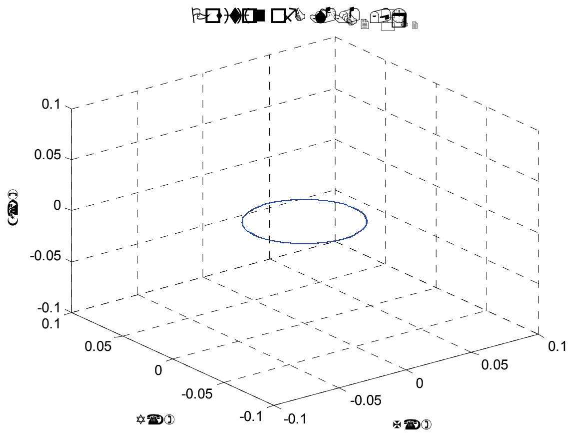

Fig. 7: Position of center of mass of link *2*.

The crank rotates at origin O_2 about *z*-axis. So the path traced by center of mass C_2 of the crank is a circle. The Fig. 7 shows the position trajectory of center of mass of crank.

3.1.2 Dynamics of connecting rod

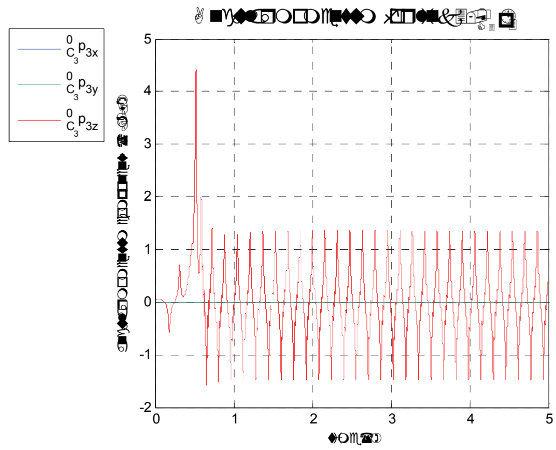

Fig. 8 : Variation of angular momentum of connecting rod with time.

The link *3*, which is connecting rod, is the link between frame *4* and crank *2*. The variation of its angular momentum with time is shown in Fig. *8*. The angular momentum increases due to the constant torque applied on crank.

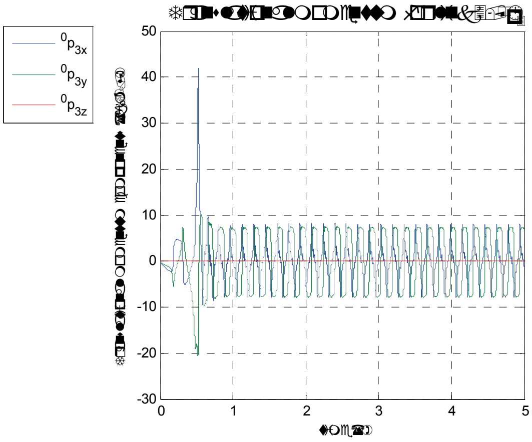

Fig. 9: Variation of Translational momentum of link *3* with time.

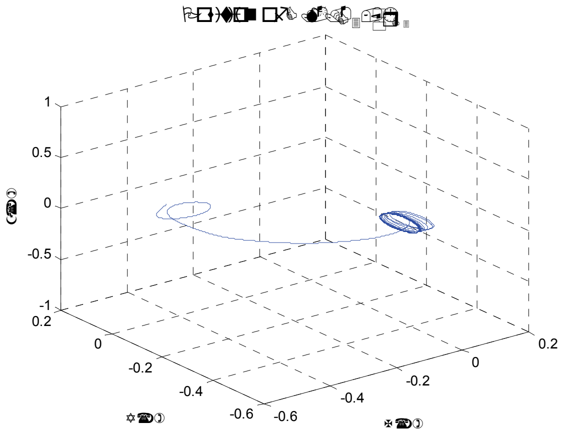

Fig. 10: Position of center of mass of link *3*.

The connecting rod oscillates and also moves up and down. The movement of the center of mass of link *3*, C_3, is represented by Fig.*10*.

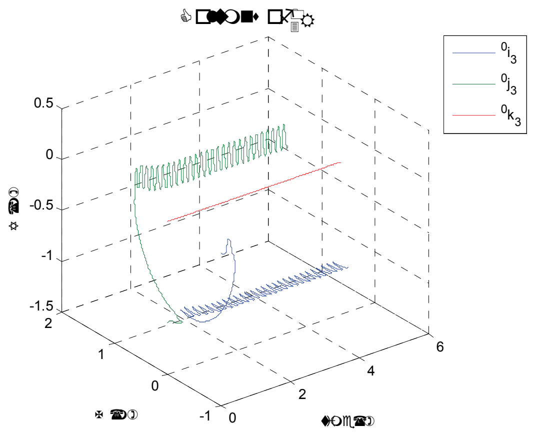

Fig. 11: Variation of orientation matrix of link *3* with time.

The movement of the connecting rod is only in *x* and *y* directions, but in *z* direction the position does not change. The connecting rod oscillates about *z* - axis. This variation is shown in graph Fig.11.

3.1.3 Dynamics of Frame

The link *4* is the frame in which the cutting blade is adjusted. The frame slides in guide ways of link *5*, in forward and backward direction and provides movement to the cutting blade for cutting operation.

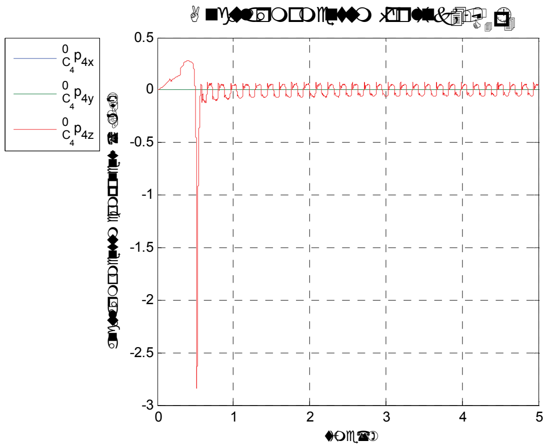

Fig. 12: Variation of angular momentum of link *4* with time.

The angular momentum changes with time at link *4*. This change is shown in Fig. *12*.

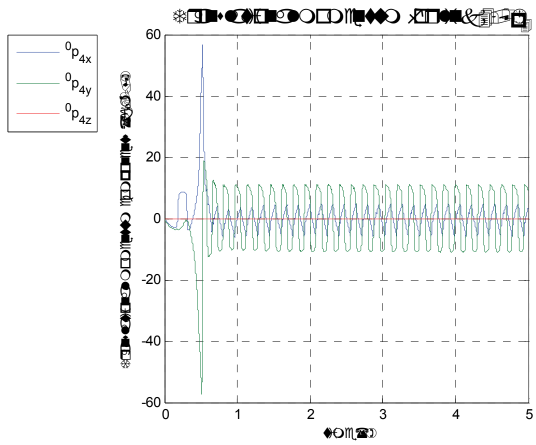

Fig. 13: Variation of Translational momentum of link *4* with time.

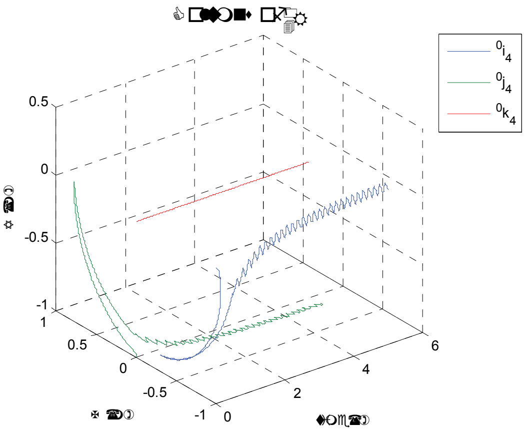

Fig. 14: Variation of orientation matrix of link *4* with time.

The frame *4* has sliding movement in the guide ways (link *5*) in *x* direction (forward and backward) and due to downward movement of link *5*, the frame *4* also moves downward. So the variation in *x* and *y* direction is shown in graph while the orientation in *z* direction does not change so the graph shows the *z* direction as a straight line.

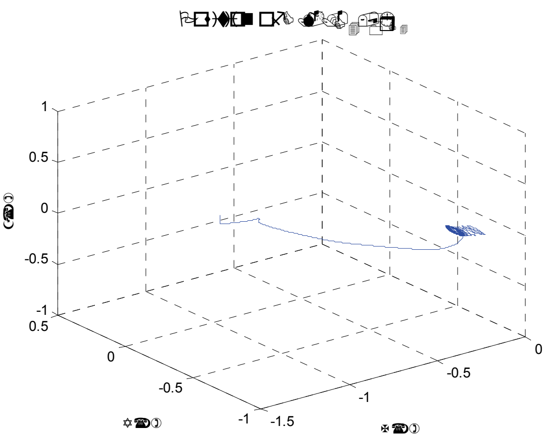

Figure 15: Position of center of mass of link *4*.

The movement of the frame *4* is changing in *x* and *y* direction and the position of its center of mass changes accordingly as shown in Fig. 15.

3.1.4 Dynamics of Guide-way (link 5)

The guide way provides downward movement to frame *4*, due to gravitational force. A slot is designed in this link for providing sliding movement to link *4*.

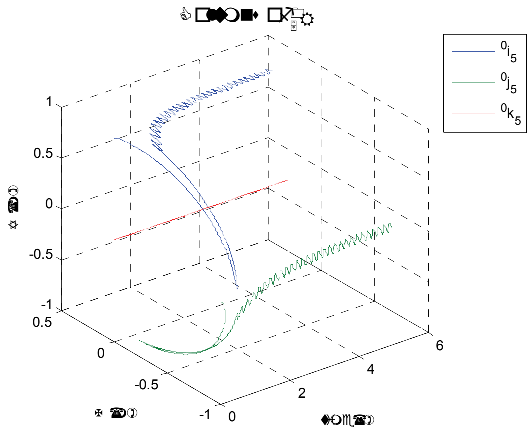

Fig. 16: Variation of orientation matrix of link *5* with time.

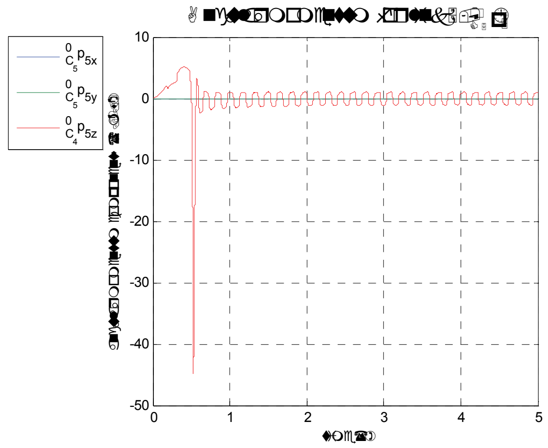

Fig. 17: Variation of angular momentum of link *5* with time.

The angular momentum of link *5* is represented in Fig. 17. The angular momentum changes sharply in the initial period due to high starting torque which is suddenly.

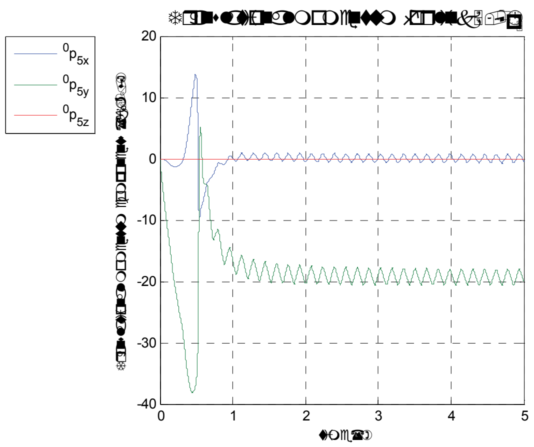

Fig. 18: Variation of Translational momentum of link *5* with time.

The position trajectory of the center of mass of the guide way link 5 is shown in Fig.19.

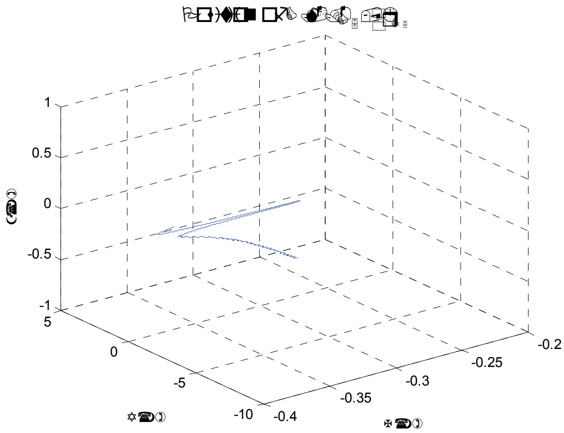

Figure 19: Position of center of mass of link *5*.

4. **Conclusions**

Dynamics of the power hacksaw machine has been modeled in this paper using bond graphs. The dynamics of the system is simulated in MATLAB, after coding directly from the Bond graph model, without deriving system equations. Simulation results agree with expected behavior. The mechanism of power hacksaw machine offers an opportunity to demonstrate multibond graph modeling of revolute as well as prismatic joints, and also the interface of the machine with work piece during the cutting operation.

REFERENCES

Bos, A. M., and Tiernego, M. J. L., 1985. Formula Manipulation in the Bond Graph Modelling and Simulation of Large Mechanical Systems," *Journal of The Franklin Institute*, 319(1/2), 51-65.

Craig, J. J., 2005. *Introduction to Robotics: Mechanics and Control*, 3rd ed. Pearson Education Inc.

Ersal, T., Stein, J. L., and Louca, L. S., 2004. A Bond Graph Based Modular Modeling Approach towards an Automated Modeling Environment for Reconfigurable Machine Tools. *The International Conference on Integrated Modeling & Analysis in Applied Control & Automation*. Paper ID IMAACA BG-06, October 28-31, Genoa, Italy.

Fu, K. S., Gonzalez, R. C., and Lee, C. S., 1987. *Robotics: Control, sensing, vision and intelligence*. McGraw Hill Book Publishing Company.

Jang, J., and Han, C., 1998. Proposition of a Modeling Method for Constrained Mechanical Systems Based on the Vector Bond Graph. *J. Franklin Institute*. 335B (3), 451-469.

Karnopp, D. C., Rosenberg, R. C., Margolis, D. L., 1990. *System Dynamics: A Unified Approach.* New York: John-Wiley and Sons Inc.

Karnopp, D. C., 1997. Understanding Multibody Dynamics Using Bond Graph representations. *J. Franklin Institute*, 334B (4), 641-642.

MATLAB, 2010. Available from: http://www.mathworks.com [accessed March, 2011]

Mukherjee, A., and Karmakar, R., 2000. *Modeling and Simulation of Engineering System through Bond Graphs*. New Delhi: Narosa Publishing House.

Murray, R. M., Li, Z., and Sastry, S. S., 1993. *A Mathematical Introduction to Robotic Manipulation*. Florida: CRC Press.

Tiernego, M. J. L., and Bos, A. M., 1985. Modelling the dynamics and Kinematics of Mechanical Systems with Multibond Graphs. *Journal of The Franklin Institute*, 319(1/2), 37-50.

Vaz, A., 2003. *Lecture Notes: Bond graph modeling for Rigid Body Dynamics*. NIT Jalandhar, India.

Vaz, A., 2004. Modeling a Hand Prosthesis with Word Bond Graph Objects. *The International Conference on Integrated Modeling & Analysis in Applied Control & Automation*. Paper ID IMAACA BG-08, October 28-31, Genoa, Italy.

Vaz, A., 2008. A Bond Graph Perspective of Computational issues in Multibody Mechanics. *Proceedings of National Conference on Mechanisms, Science and Technology from Theory to Application*, Nov. 13-14, Hamirpur, India.

Vaz, A., Sharma, P., and Atri, R., 2009. Modeling and Simulation of the Dynamics of Crankshaft-Connecting Rod-Piston-Cylinder Mechanism and a Universal Joint Using The Bond Graph Approach. 14*th National Conference on Machines and Mechanisms (NaCoMM09)*, December 17-18, NIT, Durgapur, India.

Vaz, A., and Thommen G. K., 2010. Modeling and Simulation of dynamics of the quick return Mechanisms: A Bond Graph Approach. *10th National Conference on Industrial Problems on Machines and Mechanisms (IPRoMM)*, December.